


 Cite this: *RSC Adv.*, 2022, 12, 30457

# Semi-quantitative analysis of nickel: counting-based $\mu$ PADs built *via* hand drawing and yellow oily double-sided adhesive tape

 Jian Wang, Tong Yang, Zhengjia Li, Kecen Zhou, Bo Xiao and Peng Yu \*

Excess exposure to a high environmental level of nickel can cause serious harm to human health. Therefore, it is particularly necessary to develop a low-cost, fast and sensitive method for nickel assay. In this paper, novel counting-based microfluidic paper-based devices ( $\mu$ PADs) were prepared by hand drawing and yellow oily double-sided adhesive tape. The dissolved adhesive tape was used for the first time to make the hydrophobic "ink". The marker filled with the "ink" drew the desirable layout on paper followed by a drying process. The  $\mu$ PADs were constituted of one circular sample introduction zone (diameter 4.5 mm) and four circular detection zones (diameter 3 mm). The adjoining detection zones were connected by a strip channel (1.2 mm  $\times$  2 mm). The fabrication conditions were optimized and the barriers created with the marker revealed good reproducibility. The analytical performance of the developed devices was investigated for nickel assay. The  $\text{Ni}^{2+}$  standard was added to the sample introduction zone, and subsequently moved into the detection zones containing dimethylglyoxime (DMG), where it reacted with  $\text{Ni}^{2+}$  and formed a reddish pink Ni–DMG complex. Through counting the number of colored dots, the developed  $\mu$ PADs realized the semi-quantitative analysis of nickel. More importantly, the fabrication of the developed counting-based  $\mu$ PADs only used a marker and adhesive tape, possessing the advantages of instrument-free simplicity and low cost. Our method has great potential for enabling  $\mu$ PADs to be easily implemented in laboratories or research centers with limited resources.

 Received 24th June 2022  
 Accepted 11th October 2022

DOI: 10.1039/d2ra03892g

[rsc.li/rsc-advances](http://rsc.li/rsc-advances)

## Introduction

The concentration levels of heavy metals in water resources have substantially increased as a result of modern industrial activities. Heavy metals are difficult to biodegrade when they bioaccumulate in tissues.<sup>1</sup> Nickel is a kind of heavy metal that is widely used in the fields of electroplating and battery manufacturing. Although nickel ions can promote the metabolism of organisms, exposure to a high environmental level of nickel can cause nausea, vomiting, diarrhea and an increased risk of cancer in humans.<sup>2</sup> Current analytical techniques for nickel analysis include atomic absorption spectroscopy (AAS),<sup>3</sup> electrochemistry,<sup>4</sup> inductively coupled plasma atomic emission spectroscopy<sup>5</sup> and flow injection analysis.<sup>6</sup> These methods exhibit good selectivity and high sensitivity, but require sophisticated laboratory environments with trained personnel and benchtop instruments.<sup>7</sup> These limitations make the above methods unsuitable for the in-field detection of nickel. Therefore, there is an urgent need to develop a low-cost, fast and sensitive method for nickel assay.

Paper-based microfluidic analytical devices ( $\mu$ PADs) have attracted a great deal of research interest owing to their simple

fabrication, fast analysis, high throughput and low cost.  $\mu$ PADs based on colorimetric readouts have been widely reported for the determination of Ni(II) and other heavy metal ions.<sup>8–10</sup> Although colorimetric readouts can be user-friendly, quantification based on the color intensity requires the use of external devices, such as a camera and image processing software, or relies on visual detection by the naked eye, which can vary due to the perception of the user. In order to obtain a simpler readout, Cate *et al.* described distance-based  $\mu$ PADs for the measurements of heavy metals and other analytes.<sup>11,12</sup> The distance-based readout needs a ruler to measure the length of the colored band, which correlates with the analyte concentration. In addition, some  $\mu$ PADs have been combined with fluorescence and electrochemistry methods for the sensitive detection of heavy metals.<sup>13,14</sup> These methods are characterized by high sensitivity, but they require instruments such as an electrochemical workstation or a fluorescence spectrophotometer. To avoid using expensive instruments, Lewis *et al.* demonstrated a quantitative paper-based assay platform using measurements of time as the readout.<sup>15</sup> Subsequently, to further simplify the readouts and eliminate the need for a ruler or timer, counting-based  $\mu$ PADs have been developed to provide semi-quantitative results by counting the number of colored segments, zones or bars.<sup>16–20</sup> Nevertheless, these works all used expensive equipment (*i.e.*, laser cutting machine or wax printer),

School of Materials Science and Engineering, Xiangtan University, Xiangtan 411105, China. E-mail: yupeng@xtu.edu.cn



limiting the wide application of  $\mu$ PADs in less developed and remote regions. Therefore, it is challenging to develop a low-cost and instrument-free strategy for fabricating counting-based  $\mu$ PADs that are capable of semi-quantitative detection of nickel.

A fabrication method for  $\mu$ PADs based on pen-on-paper (PoP) has emerged as a simple, low-cost alternative approach for manufacturing hydrophobic barriers on paper substrates. Whitesides *et al.* used a desktop plotter to pattern filter paper with a modified pen filled with an “ink” of polydimethylsiloxane (PDMS) diluted 3 : 1 (w/w) in hexane.<sup>21</sup> Lu *et al.* presented a simple and low-cost production method to generate  $\mu$ PADs by painting with a wax pen. The fabrication process was user-friendly and could be finished within 5–10 minutes without the need for a clean room, UV lamp or organic solvent.<sup>22</sup> Wang *et al.* developed a simple and convenient strategy for  $\mu$ PADs fabrication by easy patterning of filter paper using a permanent marker.<sup>23</sup> Lucas *et al.*, for the first time, used a 3D pen equipped with an acrylic resin and a UV handheld flashlight for fabricating  $\mu$ PADs.<sup>24</sup> Although these works have made a huge contribution to the field of PoP-based  $\mu$ PADs, the hydrophobic barrier is still constructed with wax in most of the methods, which cannot support solutions such as surfactants and organic solvents.<sup>25</sup> Therefore, our group have tried to use other substances to construct the hydrophobic boundaries of  $\mu$ PADs<sup>26–30</sup> and found that adhesive tape performed very good hydrophobicity.<sup>28</sup> Inspired by this, double-sided adhesive tape could be used as the main ingredient to manufacture the ink, paving a new way for the development of the PoP fabrication strategy.

In this paper, counting-based  $\mu$ PADs were fabricated for the first time by hand drawing and yellow oily double-sided adhesive tape, and successfully used for the semi-quantitative analysis of nickel ions. A marker filled with an “ink” of double-sided adhesive tape dissolved in toluene was used to draw hydrophobic barriers on filter paper with the help of a patterned polymethyl methacrylate (PMMA) board. Dimethylglyoxime (DMG) was used as the assay reagent to react with nickel ions to form the reddish pink Ni-DMG complex. The fabrication process was simple and fast, and no expensive instruments, such as a wax printer or an ink-jet printer, were used. Through counting the number of colored dots of the  $\mu$ PADs, nickel ions were semi-quantitatively analyzed without using a camera, smartphone, ruler, timer or image processing software. Our method has great potential for enabling  $\mu$ PADs to be easily implemented in laboratories or research centers with limited resources.

## Experimental

### Materials and reagents

Whatman filter paper No. 1 was purchased from Whatman International Ltd. (Maidstone, England) and then used for  $\mu$ PADs fabrication. Yellow oily double-sided adhesive tape (brand Youbisheng, width = 40 mm) was purchased from Shengneng Packaging Co., Ltd. (Hangzhou, China). The tape was composed of a double-sided adhesive layer and a protective film. The marker (nib diameter = 0.7 mm), which was used to

draw the pattern on the filter paper, was purchased from Shenzhen Shengjie Stationery Wholesale Collection Co., Ltd.  $\text{Ni}(\text{NO}_3)_2 \cdot 6\text{H}_2\text{O}$ , toluene,  $\text{Cu}(\text{NO}_3)_2$ ,  $\text{Co}(\text{NO}_3)_2 \cdot 6\text{H}_2\text{O}$ ,  $\text{KNO}_3$ ,  $\text{Na}_2\text{SO}_4$ ,  $\text{Ca}(\text{NO}_3)_2$ ,  $\text{Mg}(\text{NO}_3)_2$ ,  $\text{Zn}(\text{NO}_3)_2 \cdot 6\text{H}_2\text{O}$ ,  $\text{Pb}(\text{NO}_3)_2$ ,  $\text{Fe}(\text{NO}_3)_3$ ,  $\text{CH}_3\text{COONa}$ ,  $\text{NaF}$ ,  $\text{NaNO}_2$  and  $\text{MgSO}_4$  of analytical grade were bought from Sinopharm Chemical Reagent Co., Ltd. (China).  $\text{Mn}(\text{NO}_3)_2$  was bought from Aladdin Reagent Company (Shanghai, China). Tris(hydroxymethyl)aminomethane was bought from Macklin Biochemical Co., Ltd. (Shanghai, China). The natural mineral water was purchased from Emeishan Yuquan Water Industry Co., Ltd.

### Fabrication of $\mu$ PADs

The preparation of the hydrophobic “ink” is depicted in Fig. 1(a). The protective film of the double-sided tape was peeled off to obtain the adhesive layer. 10 g of the adhesive was cut into small pieces and dissolved in 30 mL of toluene. The solution was stirred with a glass rod for 5 minutes and the color of the solution became yellow. The insoluble substance was filtered by filter paper to obtain the hydrophobic ink, which was filled into a marker. Fig. 1(b) describes the fabrication of  $\mu$ PADs by PoP strategy. First, the PMMA template with the specific pattern was fixed on the filter paper. The marker filled with “ink” was used to draw the hydrophobic barriers on both sides of the filter paper. After that, the filter paper with the designed pattern was dried in an oven at 90 °C for 10 minutes to obtain the  $\mu$ PADs. The developed counting-based  $\mu$ PADs contained a sample introduction zone (diameter 4.5 mm) and four circular detection zones (diameter 3 mm). The size of the connecting channel was  $1.2 \times 2$  mm. Fig. 1(c) presents the counting-based  $\mu$ PADs for nickel detection. Chitosan solution and the assay reagent were added in the four detection zones, sequentially. After drying, the nickel standard was added in the sample introduction zone. When the  $\text{Ni}^{2+}$  standard moved from the sample introduction zone to the detection zones, DMG in each detection zone reacted with  $\text{Ni}^{2+}$ . Thus, a specific number of  $\text{Ni}^{2+}$  ions were consumed and the reddish pink Ni-DMG complex was formed in the detection zone. The color change of the detection zones did not reveal a precise concentration value, but rather correlated to a concentration range. After 10 minutes, the nickel concentration could be semi-quantitatively detected by counting the number of colored dots.

### Counting-based method for nickel detection

The nickel detection principle is based on the reaction between DMG and nickel ions.<sup>12</sup> In an alkaline environment, DMG reacts with  $\text{Ni}^{2+}$  to form the reddish pink Ni-DMG complex. 50 mmol  $\text{L}^{-1}$  of DMG and 50 mmol  $\text{L}^{-1}$  of tris(hydroxy)aminomethane were dissolved in ethanol to prepare the assay reagent.<sup>26</sup> In this work, chitosan was used as an immobilization support, which has been successfully demonstrated by different authors in sensing studies on a microfluidic scale.<sup>31–33</sup> 0.5% (m/v) chitosan was added into 2% (v/v) acetic acid solution and stirred for 30 minutes to prepare a chitosan solution.<sup>34</sup> Then, 0.3  $\mu\text{L}$  of the chitosan solution was pipetted into the four detection zones. After drying at room temperature for 10 minutes, 0.3  $\mu\text{L}$  of the



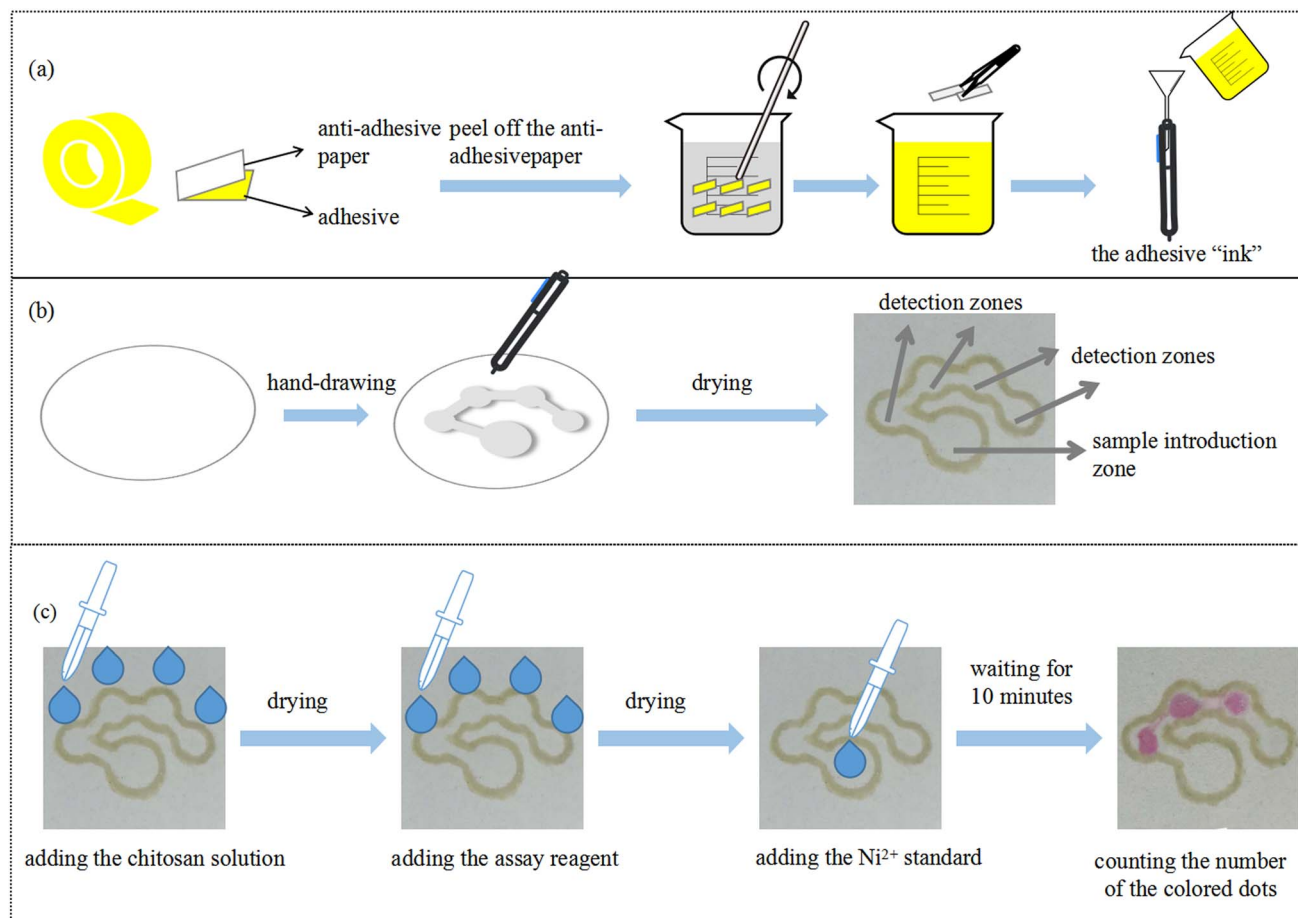


Fig. 1 (a) Preparation of the hydrophobic "ink". (b) Schematic illustration of the PoP-based fabrication process of  $\mu$ PADs. (c) The counting-based  $\mu$ PADs for nickel detection.

assay reagent was pipetted into the four detection zones and allowed to dry for 10 minutes. Finally, 12  $\mu$ L of  $Ni^{2+}$  standard solution was added to the sample introduction zone. After 10 minutes, the detection zones changed from colorless to reddish pink. The number of colored dots was observed by the naked eye. For one circular detection zone, the human eye can easily distinguish if the visualized reddish pink area accounted for half or the entire area of the detection zone. Therefore, in this work the readable number of colored dots was an integer multiple of 0.5 and the semi-quantitative analysis of  $Ni^{2+}$  could be realized by counting the number of colored dots.

### Recovery test

To evaluate the reliability and practicability of the developed  $\mu$ PADs, tap water and mineral water were used as actual samples. First, 0.3  $\mu$ L of chitosan solution and 0.3  $\mu$ L of assay reagent were added into the four detection zones and allowed to dry at room temperature for 10 minutes. Next, 12  $\mu$ L of tap water or mineral water was spiked with a series of concentrations of nickel ions and then pipetted into the sample introduction zone. The number of colored dots was counted after 10 minutes of reaction.

## Results and discussion

### The pattern design of the $\mu$ PADs

$\mu$ PADs with different patterns were constructed by PoP strategy. As shown in Fig. 2,  $\mu$ PADs with designs of parallelogram, triangle, circle, long channel and letters were successfully fabricated. After adding the red food dye solution into the hydrophilic region, no leakage was observed, indicating that the adhesive "ink" had good hydrophobic performance and the hydrophobic barrier was constructed. Therefore, the PoP-based strategy provides a simple  $\mu$ PADs fabrication technique that enables high-throughput analysis and is adaptable to different analysis methods.

### Optimization of the fabrication process

First, the marker filled with "ink" was used to draw the pattern on one or two sides of the filter paper to construct the hydrophobic barriers. After drawing, the filter paper was placed in an oven to dry at 90  $^{\circ}$ C for 10 minutes to obtain the  $\mu$ PADs. The top and bottom surface of the  $\mu$ PADs constructed by drawing on one side were photographed as shown in Fig. 3(a) and (b), respectively. The hydrophobic barrier on the bottom surface of the  $\mu$ PADs prepared by drawing patterns on one side was not



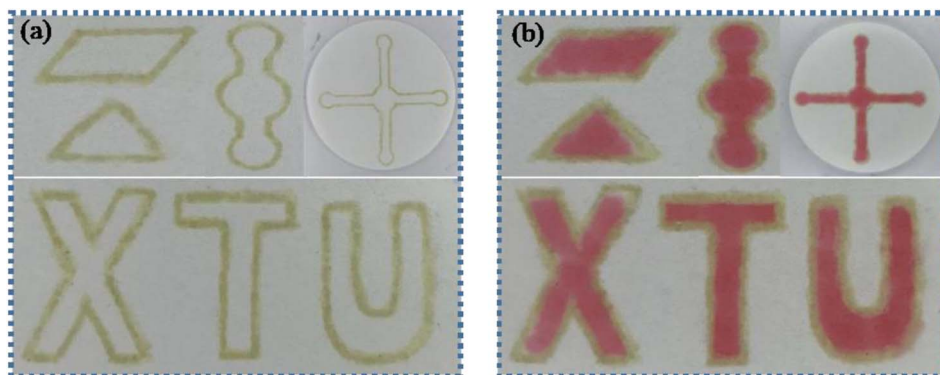


Fig. 2 (a) The developed PoP-based  $\mu$ PADs with different patterns. (b) Images of the  $\mu$ PADs after adding red food dye.

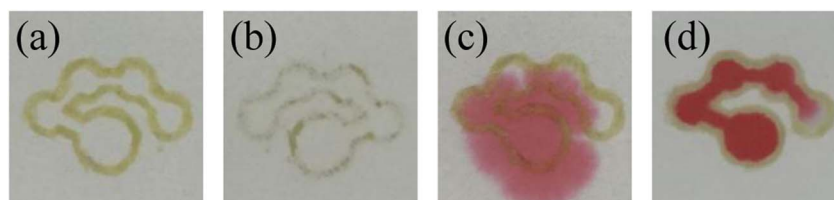


Fig. 3 The top (a) and bottom surface (b) of the single-sided drawn  $\mu$ PADs. Images of the single-sided drawn  $\mu$ PADs (c) and double-sided drawn  $\mu$ PADs (d) after adding the red food dye solution.

successfully constructed because the adhesive had not fully penetrated into the filter paper. Although the “ink” was prepared in toluene solution, the toluene volatilized quickly and reduced the fluidity of the “ink”, resulting in the incomplete penetration of the “ink” to the bottom surface of the filter paper. 12  $\mu$ L of the red food dye solution was added to the sample introduction zone of the single-sided and double-sided drawn  $\mu$ PADs to further investigate the hydrophobic performance. Images of the  $\mu$ PADs are shown in Fig. 3(c) and (d). The single-

sided drawn  $\mu$ PADs exhibited serious leakage while the double-sided drawn  $\mu$ PADs had no leakage, indicating that the “ink” had completely penetrated into the filter paper for the double-sided drawn  $\mu$ PADs and the hydrophobic barrier had been successfully constructed. Therefore, the double-sided drawing mode was used to fabricate the  $\mu$ PADs.

Then, the number of times to draw patterns on each side was optimized. The pattern was drawn once or twice on each side of the filter paper with a marker filled with “ink”. Then, the filter

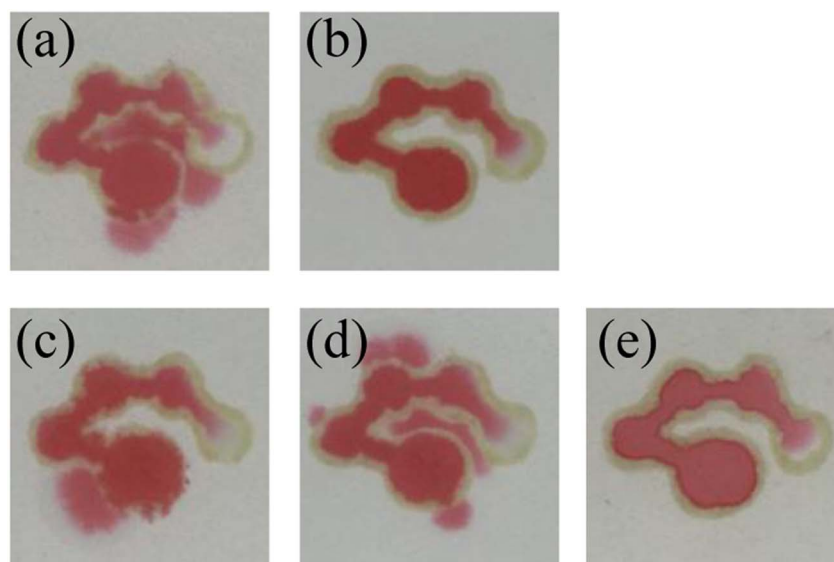


Fig. 4 A 12  $\mu$ L sample of red food dye wicks up the system of channels. Images of the  $\mu$ PADs prepared by drawing the pattern once (a) and twice (b). Images of the  $\mu$ PADs dried at room temperature (c), 60  $^{\circ}$ C (d) and 90  $^{\circ}$ C (e).





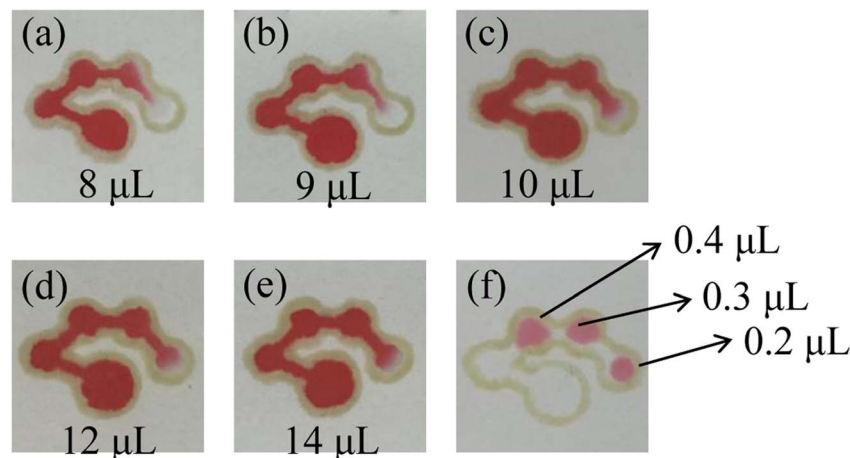


Fig. 5 Images of the  $\mu$ PADs after adding 8  $\mu$ L (a), 9  $\mu$ L (b), 10  $\mu$ L (c), 12  $\mu$ L (d) and 14  $\mu$ L (e) of the red food dye solution to the sample introduction zone and the detection zones (f).

paper with the pattern was dried in an oven at 90 °C for 10 minutes to obtain the  $\mu$ PADs. 12  $\mu$ L of the red food dye solution was added into the sample introduction zone of the  $\mu$ PADs to investigate the hydrophobic performance. As shown in Fig. 4(a), the red food dye solution leaked from the hydrophobic barrier in the  $\mu$ PADs with the pattern drawn once, indicating the poor hydrophobic property. However, the  $\mu$ PADs prepared by drawing the pattern twice showed no leakage, demonstrating that the hydrophobic barrier was successfully constructed. Therefore, drawing the pattern twice on each side was chosen for the  $\mu$ PADs fabrication process.

Finally, the drying temperature was also optimized. The developed  $\mu$ PADs were dried under a certain temperature (room temperature, 60 °C and 90 °C) for 10 minutes. Then, 12  $\mu$ L of the red food dye solution was added to the sample introduction zone, and moved through all the channels and detection zones. The results are shown in Fig. 4(c)–(e). It was observed that the  $\mu$ PADs that were dried at room temperature and 60 °C exhibited solution leakage while the  $\mu$ PADs dried at 90 °C had no leakage. The reason was that the “ink” was completely dried at 90 °C, resulting in satisfactory hydrophobic performance. Therefore, 90 °C was selected as the drying temperature.

### Optimization of sample volume

Several different sample volumes (8, 9, 10, 12 and 14  $\mu$ L) of red food dye solution were added to the sample introduction zone of the  $\mu$ PADs. After 10 minutes, the results of the fluid flow in the chip were recorded. As shown in Fig. 5(a)–(e), when 8, 9 and 10  $\mu$ L of red food dye were added, the fourth detection zone was not completely filled. After adding 12  $\mu$ L or 14  $\mu$ L of the red food dye solution, the fourth detection zone was almost filled by the solution. Therefore, the optimal volume for the sample introduction was selected to be 12  $\mu$ L. Then, the volume of the assay reagent added to the detection zone was optimized. 0.2, 0.3 and 0.4  $\mu$ L of the red food dye solution was added to the detection zones of the  $\mu$ PADs. The results are shown in Fig. 5(f). 0.2  $\mu$ L of the solution could not fill a single detection zone while 0.3  $\mu$ L could. 0.4  $\mu$ L filled both the detection zone and part of the channel, causing waste of the assay reagent. Therefore, the optimal volume of the assay reagent was selected as 0.3  $\mu$ L.

### Characterization of the $\mu$ PADs

A series of PMMA boards with the round shape (diameter = 2.4–6.0 mm) and the channels (width = 1.5–3.5 mm) were fixed on the paper surface. Hydrophobic barriers with different shapes

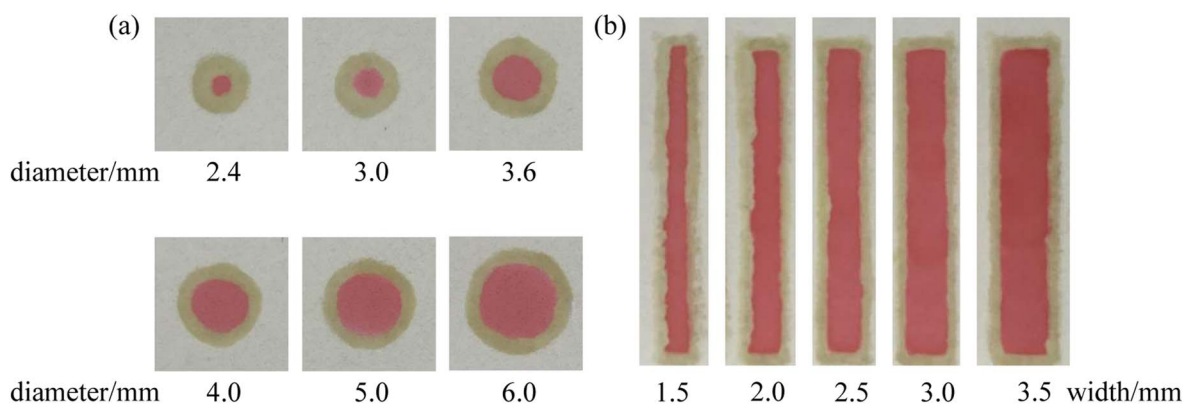


Fig. 6 Images of the developed  $\mu$ PADs with circular hydrophobic barriers (a) and rectangular hydrophobic barriers (b).



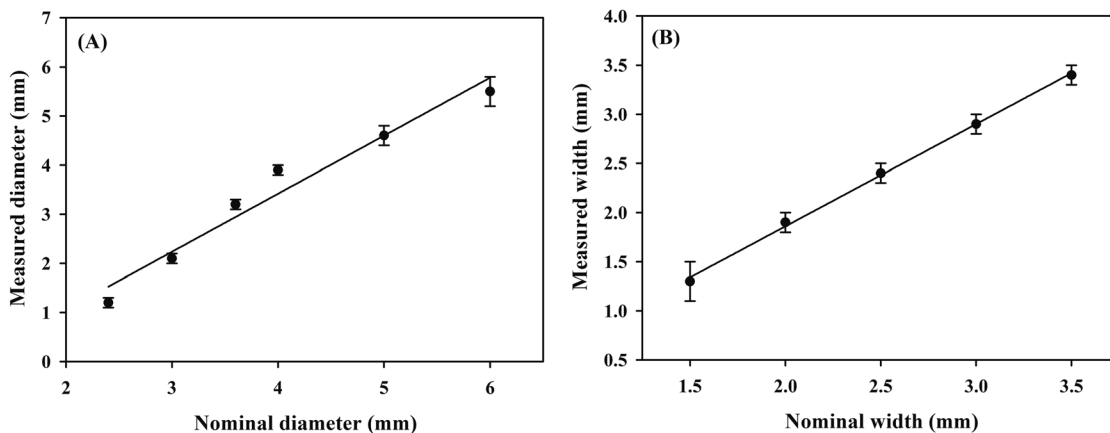


Fig. 7 The linear relationship between nominal and measured dimensions for the circle diameter (a) and the channel width (b).

were constructed with the marker filled with the adhesive “ink” with the help of the PMMA boards. Then, the red food dye solution was added to the developed  $\mu$ PADs and the photos of the  $\mu$ PADs are shown in Fig. 6. In all the  $\mu$ PADs, the hydrophobic barriers were clear, indicating that the infiltration direction of the “ink” was well controlled. The real diameters and real widths of the hydrophobic barriers were measured and the results were in good agreement with the nominal dimensions (Fig. 7). For the circles designed with diameters of 2.4, 3.0, 3.6, 4.0, 5.0 and 6.0 mm, the measured values were 1.2, 2.1, 3.2, 3.9, 4.6 and 5.5 mm, respectively. For the channels designed with widths of 1.5, 2.0, 2.5, 3.0 and 3.5 mm, the measured values were 1.3, 1.9, 2.4, 2.9 and 3.4 mm, respectively. The relative standard deviations of the measured sizes calculated for five circles (3.0, 3.6, 4.0, 5.0 and 6.0 mm) and four channels (2.0, 2.5, 3.0 and 3.5 mm) were lower than 10%. The results demonstrate that the PoP fabrication strategy based on the adhesive “ink” exhibits good reproducibility. In addition, the cost of a  $\mu$ PAD was about \$0.02. The PoP fabrication strategy did not require the use of any expensive instruments, providing an alternative method for the construction of counting-based  $\mu$ PADs with the advantages of low cost, high efficiency and simplicity.

#### Assay performance of the counting-based $\mu$ PADs for the detection of nickel

It is noted from Fig. 8 that when the nickel standard solution was added to the sample introduction zone, the color of the detection zones changed from colorless to reddish pink. It was observed that an increase in nickel concentration resulted in an

increased number of the colored dots. Fig. 9 presents the relationship between the number of colored dots and the nickel concentration. The higher the concentration of  $\text{Ni}^{2+}$ , the more colored dots in the detection zones. It could be observed by the naked eye that 0.5, 1.0, 4.0 and 8.0  $\text{mmol L}^{-1}$   $\text{Ni}^{2+}$  produced about 1.5, 2, 3 and 4 colored dots, respectively. The results demonstrate that the developed  $\mu$ PADs provides a user-friendly way to semi-quantitatively detect  $\text{Ni}^{2+}$  based on counting the colored dots. Although the assay concentration of nickel ions was at the millimolar per liter concentration level, the assay of nickel ions within low concentration levels could be possible by using a pre-concentration step or nanomaterials,<sup>35,36</sup> which we hope to explore in further work.

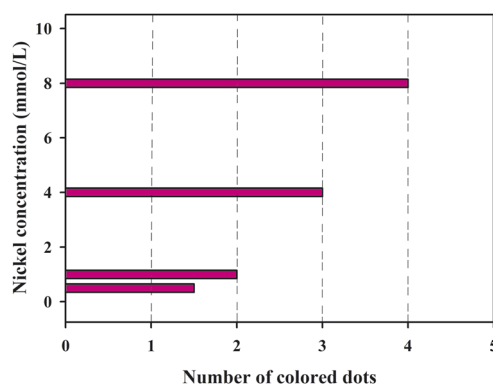


Fig. 9 The relationship between the number of colored dots and the concentration of nickel.

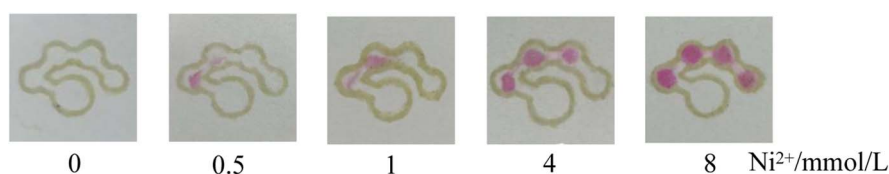


Fig. 8 Images of the counting-based  $\mu$ PADs after adding 12  $\mu\text{L}$  of different concentrations of nickel (0, 0.5, 1, 4 and 8  $\text{mmol L}^{-1}$ ) to the sample introduction zone.



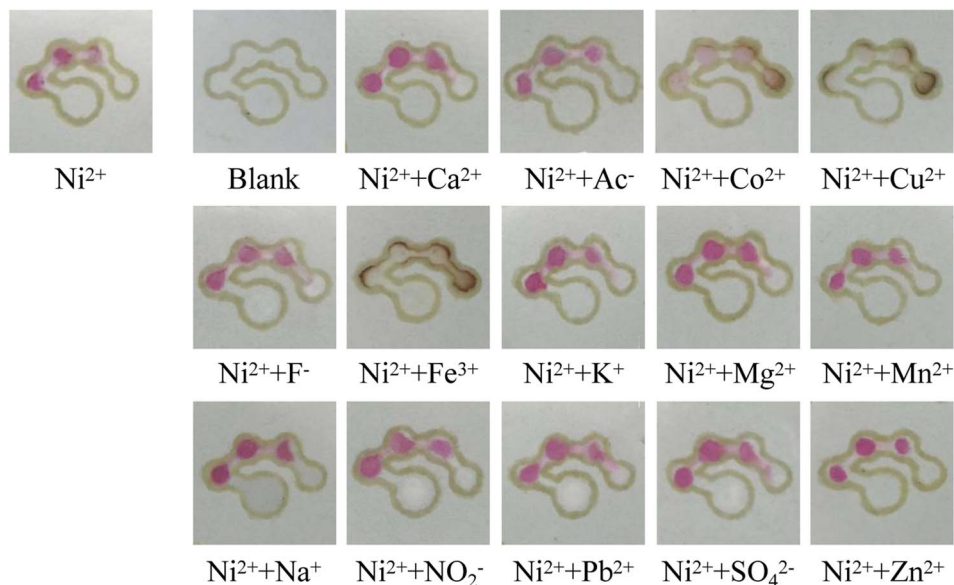


Fig. 10 Images of the counting-based  $\mu$ PADs after adding 12  $\mu$ L of the different solutions to the sample introduction zone.

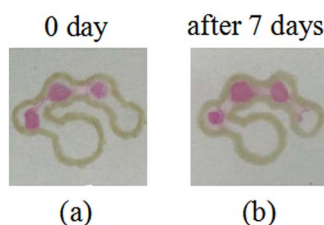


Fig. 11 Images of the counting-based  $\mu$ PADs after adding 12  $\mu$ L of 4  $\text{mmol L}^{-1}$   $\text{Ni}^{2+}$  to the sample introduction zone: (a) freshly prepared  $\mu$ PADs (0 day) and (b)  $\mu$ PADs stored for 7 days.

#### The specificity and stability of the $\mu$ PADs

The specificity of the  $\mu$ PADs was investigated. Common ions such as  $\text{Cu}^{2+}$ ,  $\text{Co}^{2+}$ ,  $\text{K}^+$ ,  $\text{Na}^+$ ,  $\text{Ca}^{2+}$ ,  $\text{Mg}^{2+}$ ,  $\text{Zn}^{2+}$ ,  $\text{Mn}^{2+}$ ,  $\text{Pb}^{2+}$ ,  $\text{Fe}^{3+}$ ,  $\text{CH}_3\text{COO}^-$ ,  $\text{F}^-$ ,  $\text{NO}_2^{2-}$  and  $\text{SO}_4^{2-}$  were selected as the interferents.<sup>8,37</sup> A series of mixed solutions containing 40  $\text{mmol L}^{-1}$  of one kind of interfering ion and 4  $\text{mmol L}^{-1}$  of nickel standard were prepared. 12  $\mu$ L of the mixed solution was added to the sample introduction zone of the  $\mu$ PADs and the number of colored dots was observed by the naked eye. The results are shown in Fig. 10. It is noted that most of the interfering ions had no influence on the detection of nickel by the counting-based  $\mu$ PADs. However, in the presence of  $\text{Co}^{2+}$ ,  $\text{Cu}^{2+}$  and

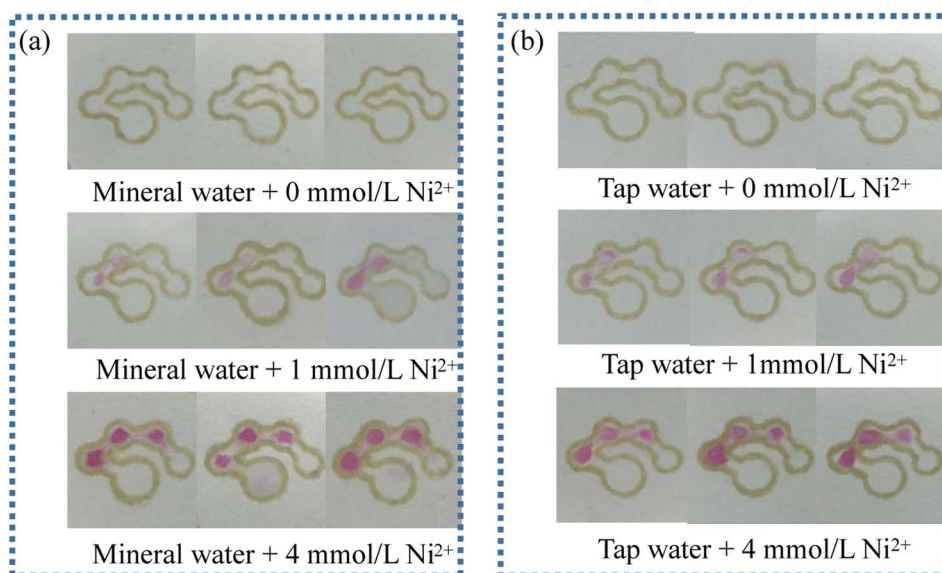


Fig. 12 Images of the counting-based  $\mu$ PADs after adding 12  $\mu$ L of mineral water (a) and tap water (b) spiked with 0, 1 and 4  $\text{mmol L}^{-1}$   $\text{Ni}^{2+}$  standard.



$\text{Fe}^{3+}$ , the number of colored dots increased from three to four, and the detection zones changed to a brown color, indicating that these metal ions could react with DMG to generate a complex. In order to avoid the interference of these ions, NaF could be used to mask  $\text{CO}^{2+}$  and  $\text{Fe}^{3+}$ , and  $\text{Na}_2\text{S}_2\text{O}_3$  could be used for masking  $\text{Cu}^{2+}$ .<sup>10</sup>

The stability of the counting-based  $\mu\text{PADs}$  was evaluated. After adding 0.3  $\mu\text{L}$  of 0.5% (m/v) chitosan solution and 0.3  $\mu\text{L}$  of the assay reagent to the four detection zones of the  $\mu\text{PADs}$ , the  $\mu\text{PADs}$  were placed in a refrigerator at 4 °C for 7 days. Then, 12  $\mu\text{L}$  of 4 mmol  $\text{L}^{-1}$   $\text{Ni}^{2+}$  standard was added to the sample introduction zone. After 10 minutes of reaction, the number of colored dots was observed by the naked eye. As shown in Fig. 11, there was no significant difference in the number of colored dots between the freshly prepared  $\mu\text{PADs}$  (0 days) and the  $\mu\text{PADs}$  stored for 7 days, indicating that the  $\mu\text{PADs}$  have good stability.

### Recovery test

The practicability and reliability of the fabricated  $\mu\text{PADs}$  were evaluated with tap water and mineral water as real samples. The results are shown in Fig. 12. The number of colored dots was basically the same as that for the nickel standard prepared with the distilled water. In addition, there was no significant difference in the number of colored dots in the same set of parallel trials, indicating good reproducibility. Therefore, it can be concluded that the counting-based method has good reliability and practicability, and can thus be used for the detection of nickel in real samples.

## Conclusions

In this paper, dot-counting-based  $\mu\text{PADs}$  for the semi-quantitative analysis of nickel have been successfully constructed by using yellow oily double-sided adhesive tape. The adhesive tape was dissolved in toluene to prepare a hydrophobic “ink”, which was filled in a marker. With the help of the PMMA template, the contour of the pattern was drawn on the filter paper with a marker to construct the hydrophobic barrier. Thereby the hydrophilic and hydrophobic regions of the  $\mu\text{PADs}$  were defined. The fabrication process was simple and fast, and no expensive instruments such as a wax printer or an ink-jet printer were used. Through counting the number of colored dots of the  $\mu\text{PADs}$ , nickel ion was semi-quantitatively analyzed without the need for a camera, smart phone, ruler, timer or image processing software. The  $\mu\text{PADs}$  exhibited good specificity and stability. More importantly, by changing the designed pattern, the adhesive-based PoP fabrication strategy could be easily extended to construct  $\mu\text{PADs}$  that are suitable for different assay methods and the detection of other analytes.

## Conflicts of interest

There are no conflicts to declare.

## Acknowledgements

The authors are grateful for the financial support from the National Innovation Training Program for college students (grant number 202110530018) and the National Natural Science Foundation of China (grant number 21804114).

## References

- 1 A. Ensafi, A. R. Allafchian and B. Rezaei, *J. Braz. Chem. Soc.*, 2015, **26**, 1482–1490.
- 2 G. K. Bielmyer, M. Grosell and K. V. Brix, *Environ. Sci. Technol.*, 2006, **40**, 2063–2068.
- 3 C. Duran, A. Gundogdu, V. N. Bulut, M. Soylak, L. Elci, H. B. Sentürk and M. Tüfekci, *J. Hazard. Mater.*, 2007, **146**, 347–355.
- 4 H. Sopha, V. Jovanovski, S. B. Hocevar and B. Ogorevc, *Electrochem. Commun.*, 2012, **20**, 23–25.
- 5 Y. Xu, J. Zhou, G. Wang, J. Zhou and G. Tao, *Anal. Chim. Acta*, 2007, **584**, 204–209.
- 6 D. Vendramini, V. Grassi and E. A. G. Zagatto, *Anal. Chim. Acta*, 2006, **570**, 124–128.
- 7 Y. Bhattacharjee and A. Chakraborty, *ACS Sustainable Chem. Eng.*, 2014, **2**, 2149–2154.
- 8 H. Wang, Y. Li, J. Wei, J. Xu, Y. Wang and G. Zheng, *Anal. Bioanal. Chem.*, 2014, **406**, 2799–2807.
- 9 A. R. Allafchian, B. Farajmand and A. J. Koupaei, *Bull. Environ. Contam. Toxicol.*, 2018, **100**, 529–535.
- 10 X. Sun, B. Li, A. Qi, C. Tia, J. Han, Y. Shi, B. Lin and L. Chen, *Talanta*, 2018, **178**, 426–431.
- 11 D. M. Cate, S. D. Noblitt, J. Volckens and C. S. Henry, *Lab Chip*, 2015, **15**, 2808–2818.
- 12 D. M. Cate, W. Dungchai, J. C. Cunningham, J. Volckens and C. S. Henry, *Lab Chip*, 2013, **13**, 2397–2404.
- 13 J. Zhou, B. Li, A. Qi, Y. Shi, J. Qi, H. Xu and L. Chen, *Sens. Actuators, B*, 2020, **305**, 127462.
- 14 J. Shi, F. Tang, H. Xing, H. Zheng, L. Bi and W. Wang, *J. Braz. Chem. Soc.*, 2012, **23**, 1124–1130.
- 15 G. G. Lewis, J. S. Robbins and S. T. Phillips, *Anal. Chem.*, 2013, **85**, 10432–10439.
- 16 S. Karita and T. Kaneta, *Anal. Chim. Acta*, 2016, **924**, 60–67.
- 17 S. G. Jeong, S. H. Lee, C. H. Choi, J. Kim and C. S. Lee, *Lab Chip*, 2015, **15**, 1188–1194.
- 18 S. Karita and T. Kaneta, *Anal. Chem.*, 2014, **86**, 12108–12114.
- 19 Y. Zhang, C. Zhou, J. Nie, S. Le, Q. Qin, F. Liu, Y. Li and J. Li, *Anal. Chem.*, 2014, **86**, 2005–2012.
- 20 M. A. Mahmud, E. J. M. Blondeel and B. D. MacDonald, *Biomicrofluidics*, 2020, **14**, 014107.
- 21 D. A. Bruzewicz, M. Reches and G. M. Whitesides, *Anal. Chem.*, 2008, **80**, 3387–3392.
- 22 Y. Lu, W. Shi, L. Jiang, J. Qin and B. Lin, *Electrophoresis*, 2009, **30**, 1497–1500.
- 23 B. Wang, Z. Lin and M. Wang, *J. Chem. Educ.*, 2015, **92**, 733–736.
- 24 L. R. Sousa, L. C. Duarte and W. K. T. Coltro, *Sens. Actuators, B*, 2020, **312**, 128018.





## Paper

- 25 T. M. G. Cardoso, F. R. de Souza, P. T. Garcia, D. Rabelo, C. S. Henry and W. K. T. Coltro, *Anal. Chim. Acta*, 2017, **974**, 63–68.
- 26 B. Nie, S. Zhao, M. Deng, P. Yu, Y. Yang, W. Lei and L. Yin, *J. Braz. Chem. Soc.*, 2021, **32**, 599–608.
- 27 P. Yu, M. Deng, Y. Yang, B. Nie and S. Zhao, *Sensors*, 2020, **20**, 4118.
- 28 P. Yu, M. Deng and Y. Yang, *Sensors*, 2019, **19**, 4082.
- 29 M. Deng, C. Liao, X. Wang, S. Chen, F. Qi, X. Zhao and P. Yu, *Can. J. Chem.*, 2019, **97**, 373–377.
- 30 G. L. Xie, H. Yu, M. H. Deng, X. L. Zhao and P. Yu, *Chem. Pap.*, 2019, **73**, 1509–1517.
- 31 W. Liu, C. L. Cassano, X. Xu and Z. H. Fan, *Anal. Chem.*, 2013, **85**, 10270–10276.
- 32 S. Wang, L. Ge, X. Song, J. Yu, S. Ge, J. Huang and F. Zeng, *Biosens. Bioelectron.*, 2012, **31**, 212–218.
- 33 V. Vosmanska, K. Kolarova, S. Rimpelova, Z. Kolska and V. Svorcik, *RSC Adv.*, 2015, **5**, 17690–17699.
- 34 E. F. M. Gabriel, P. T. Garcia, T. M. G. Cardoso, F. M. Lopes, F. T. Martins and W. K. T. Coltro, *Analyst*, 2016, **141**, 4749–4756.
- 35 A. Rossi, M. Zannotti, M. Cuccioloni, M. Minicucci, . Petetta, M. Angeletti and R. Giovannetti, *Nanomaterials*, 2021, **11**, 1733.
- 36 M. Annadhasan, J. Kasthuri and N. Rajendiran, *RSC Adv.*, 2015, **5**, 11458–11468.
- 37 H. Zare, M. Ghalkhani, O. Akhavan, N. Taghavinia and M. Marandi, *Mater. Res. Bull.*, 2017, **95**, 532–538.

